Computer Simulation Study of Stiffness Variation of Stewart Platform under Different Loads

Zhiqiang Zhao*, Yuetao Liu*, Changsong Yu, Peicen Jiang
School of Mechanical Engineering, Shandong University of Technology, Zibo 255000, China

***Abstract*—The ability of Stewart platform to resist deformation is an important target for designing and optimizing the platform, and studying the variation rule of stiffness of Stewart platform under different loads can help us to understand the dynamic characteristics of the platform, guide the design and control of the platform, and improve the performance and stability of the platform. The purpose of this paper is to change the law of stiffness variation and influence factors of Stewart platform under different loads, aiming to study the change of stiffness of Stewart platform under different loads as well as the influence factors, and the influence of stiffness change on the performance and stability of the platform. Firstly, using MATLAB software, the kinematic and mechanical model of Stewart platform was established, the analytical expression of the stiffness matrix of the platform was deduced, and the stiffness characteristics and stiffness singularity of the platform were analyzed. Then, using ADAMS software, the dynamic simulation model of the Stewart platform was established, and the stiffness of the platform was simulated and analyzed. The results show that the stiffness of the Stewart platform will appear singularity or sudden change under some special positions or loads, which should be avoided as much as possible so as not to affect the performance and stability of the platform. There is a certain correlation between the dynamic and static stiffness, but it is also affected by the nonlinearity of the structure, damping, coupling and other factors.**

***Keywords*—Stewart; different loads; stiffness variation; computer simulation**

I. Introduction

The Stewart platform is a parallel mechanism consisting of six retractable legs connecting a fixed abutment and a moving platform, which can realize the control of the platform's arbitrary position in three-dimensional space [1]. The Stewart platform was initially invented by Gough in 1947 for detecting the wear and tear of tires, and was later proposed by Stewart in 1965 to be applied to flight simulators, thus attracting much attention and research [2, 3].

The stiffness of Stewart platform refers to the ability of the platform to resist deformation, which is an important parameter affecting the performance of the platform, and also an important target for the design and optimization of the platform. The stiffness of Stewart platform is affected by a variety of factors, such as the length of the legs, angle, cross-section, material, etc., as well as the platform's position, load, speed, etc. The stiffness problem of Stewart platform has the characteristics of nonlinear, strong coupling, multi-variable, etc., so its analysis and calculation is a challenging work. And strong coupling, multivariate and so on, so its analysis and calculation is a challenging work. Studying the variation rule of the stiffness of Stewart platform under different loads can help us understand the dynamic characteristics of the platform, guide the design and control of the platform, and improve the performance and stability of the platform [4].

The main research content of this paper is to explore the change rule of stiffness and influence factors of Stewart platform under different loads, aiming to study the change of stiffness of Stewart platform under different loads as well as the influence factors, and the influence of stiffness change on the performance and stability of the platform [5, 6].

The following two hypotheses exist for the study of this paper:

H0: The stiffness of the Stewart platform under different loads varies with the length, angle, cross-section and material of the outriggers [7, 8].

H1: Changes in stiffness will affect the platform's response speed, accuracy, anti-interference ability, etc., thus affecting the platform's performance and stability.

In order to solve the above problems, this paper aims to establish the dynamics model and computer simulation model of Stewart platform, analyze the stiffness variation rules and influencing factors of Stewart platform under different loads through simulation experiments, and assess the influence of stiffness variation on the performance and stability of the platform [9].

In this paper, a six-degree-of-freedom Stewart platform is used as the object of study, assuming that the platform abutment and the platform are rigid bodies, the cross-section of the outrigger is circular, the extension and retraction of the outrigger is driven by an electric motor, the load of the platform is a mass, the motion of the platform is controlled by the given bit-positioning trajectory, and the stiffness of the platform is defined by the ratio of the platform's displacements to its forces [10].

II. Literature Review

Eftekhari and Karimpour [11] reviewed the current status and progress of research on the stiffness and statics of parallel robots, including the concept, classification, calculation method, change rule, and optimal design of stiffness, as well as the basic principles, analysis methods, and control strategies of statics. Gallardo and Alcaraz [12] proposed a stiffness optimization design method based on genetic algorithm to maximize or minimize the stiffness of the platform by changing the length and layout of the legs. Hauenstein et al.

[13] proposed a fuzzy logic-based stiffness control method to make the stiffness of the platform adjustable by adjusting the length and speed of the outriggers to adapt to different working conditions and task requirements. He et al. [14] adopted the Monte Carlo method to analyze the stiffness sensitivity of the Stewart platform, and the degree and direction of the influence of the length, angle, cross-section and material of the outrigger on the platform stiffness were examined, and the sensitivity coefficient and sensitivity index of the platform stiffness were obtained.

He et al. [15] used ADAMS software to establish the dynamic simulation model of Stewart platform, and simulated and analyzed the platform stiffness, and obtained the change curves of the platform stiffness with the factors of the position, load, speed, etc., and compared and verified the results with the theoretical analysis. Hu and Jing [16] analyzed the sources and effects of the stiffness error of the Stewart platform, including the length error, angle error, cross-section error and material error of the outrigger, etc. The mathematical model of the platform stiffness error is established, the magnitude and the direction of the platform stiffness error are calculated, and a stiffness error compensation method based on the feedback control is put forward, in which the stiffness error of the platform is minimized by adjusting the length and the speed of the outrigger. Huang et al. [17] established a multi-objective optimization problem by comprehensively considering the platform's performance indexes such as stiffness, load capacity and workspace, and a multi-objective genetic algorithm was adopted to optimize the platform's design variables such as geometrical parameters, outrigger materials, connection methods, etc., and a set of optimal solutions balancing various performance indexes was obtained to evaluate the platform's stiffness performance, which was compared and analyzed with that of other platforms [18, 19].

These literatures mainly focus on the theoretical analysis, numerical simulation, simulation verification and optimization design of the stiffness performance of the Stewart platform, covering the calculation method of the stiffness, change rule, control strategy, sensitivity analysis, error compensation, etc., which provide valuable references for the application of the Stewart platform. However, the AI-based Stewart platform lacks experimental verification of the stiffness change under different loads, and cannot fully consider the influence of various uncertainties in the actual working environment, such as temperature, humidity, vibration, etc., on the stiffness of the platform. In addition, the stiffness control method of the AI-based Stewart platform needs to be further improved [20].

The main deficiencies of the current Stewart platform research are the lack of sufficient real-world validation, especially for the AI-driven stiffness control system; the lack of comprehensive consideration of the impact of uncertain factors such as temperature, humidity, and vibration on the platform stiffness in the actual working environment; and the optimization of algorithms for the dynamic adaptability and long-term stability that still needs to be strengthened. To overcome these problems, the following strategies are suggested: first, enhance the experimental validation link by building physical prototypes and deploying them in diverse real-world application scenarios to collect comprehensive stiffness change data to ensure that the theoretical model matches the real-world performance; second, incorporate environment-aware technologies, use sensor networks to monitor changes in external conditions in real time, and integrate these data into AI algorithms to enable the platform to dynamically Finally, promote algorithmic innovation, especially the use of advanced AI technologies such as reinforcement learning, so that the platform can self-learn and optimize control strategies to maintain high performance and stability in complex and changing environments, to ensure that the research results are more in line with the actual needs and to promote technological progress.

III. Simulation Study on the Stiffness Change of Stewart Platform under Different Loads

In order to analyze the stiffness variation characteristics of the Stewart platform under different loads, the stiffness of the Stewart platform was simulated and analyzed in this paper using MATLAB and ADAMS software [21]. Firstly, using MATLAB software, the kinematic and mechanical models of the Stewart platform were established, the analytical expression of the stiffness matrix of the platform was derived, and the stiffness characteristics and stiffness singularity of the platform were analyzed. Then, using ADAMS software, the dynamic simulation model of the Stewart platform was established, and the stiffness of the platform was simulated and analyzed, which was compared and verified with the theoretical analysis results [22].

A. Theoretical Models

The Stewart platform is a six-degree-of-freedom parallel mechanism consisting of an upper platform and a lower platform, and the two platforms are connected to each other by six legs, each of which consists of a ball hinge and a universal joint, as shown in Fig. 1.

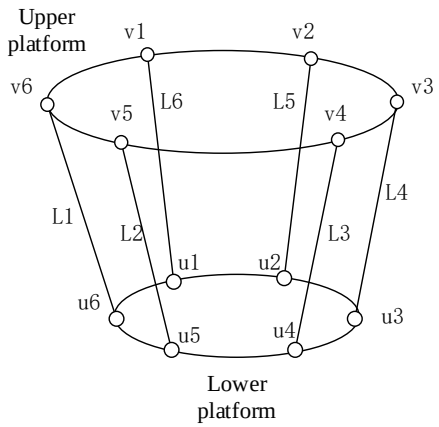

Fig. 1. Parallel mechanism with six degrees of freedom.

In the body coordinate system, the position vector of the center of mass of the upper platform and the position vector of the center of mass to the th hinge point are shown in Equation (1). In the body coordinate system , the position vector of the center of mass of the lower platform and the position vector of the center of mass to the th hinge point are shown in Equation (2) [23, 24].

$$\mathbf{r}_{ao}=\begin{bmatrix}x_a\\y_a\\z_a\end{bmatrix},\quad \mathbf{a}_i=\begin{bmatrix}r_a\cos(\alpha_1+(i-1)\alpha)\\r_a\sin(\alpha_1+(i-1)\alpha)\\0\end{bmatrix},\quad i=1,2,\ldots,6 \tag{1}$$

$$\mathbf{r}_{bo}=\begin{bmatrix}x_b\\y_b\\z_b\end{bmatrix},\quad \mathbf{b}_i=\begin{bmatrix}r_b\cos(\beta_1+(i-1)\beta)\\r_b\sin(\beta_1+(i-1)\beta)\\0\end{bmatrix},\quad i=1,2,\ldots,6 \tag{2}$$

After coordinate transformation, the position vectors $\mathbf{a}_i$, $\mathbf{b}_i$ to the reference coordinate system can be expressed as $\mathbf{a}_i^g=\mathbf{r}_{ao}^g+R_a\mathbf{a}_i$, $\mathbf{b}_i^g=\mathbf{r}_{bo}^g+R_b\mathbf{b}_i$, where R_a, R_b denote the transformation matrix from the body coordinate system $O_aX_aY_aZ_a$, $O_bX_bY_bZ_b$ to the reference coordinate system $O_gX_gY_gZ_g$ respectively. R_a, the expression of R_b is shown in Equation (3) and Equation (4) [25].

$$R_a=\begin{bmatrix}c_{\alpha_a}c_{\beta_a} & c_{\alpha_a}s_{\beta_a}s_{\gamma_a}-s_{\alpha_a}c_{\gamma_a} & c_{\alpha_a}s_{\beta_a}c_{\gamma_a}+s_{\alpha_a}s_{\gamma_a}\\ s_{\alpha_a}c_{\beta_a} & s_{\alpha_a}s_{\beta_a}s_{\gamma_a}+c_{\alpha_a}c_{\gamma_a} & s_{\alpha_a}s_{\beta_a}c_{\gamma_a}-c_{\alpha_a}s_{\gamma_a}\\ -s_{\beta_a} & c_{\beta_a}s_{\gamma_a} & c_{\beta_a}c_{\gamma_a}\end{bmatrix} \tag{3}$$

$$R_b=\begin{bmatrix}c_{\alpha_b}c_{\beta_b} & c_{\alpha_b}s_{\beta_b}s_{\gamma_b}-s_{\alpha_b}c_{\gamma_b} & c_{\alpha_b}s_{\beta_b}c_{\gamma_b}+s_{\alpha_b}s_{\gamma_b}\\ s_{\alpha_b}c_{\beta_b} & s_{\alpha_b}s_{\beta_b}s_{\gamma_b}+c_{\alpha_b}c_{\gamma_b} & s_{\alpha_b}s_{\beta_b}c_{\gamma_b}-c_{\alpha_b}s_{\gamma_b}\\ -s_{\beta_b} & c_{\beta_b}s_{\gamma_b} & c_{\beta_b}c_{\gamma_b}\end{bmatrix} \tag{4}$$

Where $(\alpha_a,\beta_a,\gamma_a)$ and $(\alpha_b,\beta_b,\gamma_b)$ denote the angle between the axes of the upper and lower platform body coordinate system and the reference coordinate system, respectively. $\mathbf{L}_i=\mathbf{a}_i^g-\mathbf{b}_i^g$, $i=1,2,\ldots,6$, the length of the leg L_i is obtained as $l_i=\|\mathbf{L}_i\|$, $i=1,2,\ldots,6$. According to the kinematic constraints of the Stewart platform, it can be obtained as $\mathbf{L}_i^T\mathbf{L}_i=l_i^2$, $i=1,2,\ldots,6$. Substituting the expressions of $\mathbf{r}_{ao}^g$, $\mathbf{r}_{bo}^g$, R_a and R_b into the above equation, the expression shown in Equation (5) can be obtained.

$$\begin{bmatrix}x_a\\y_a\\z_a\\\alpha_a\\\beta_a\\\gamma_a\\x_b\\y_b\\z_b\\\alpha_b\\\beta_b\\\gamma_b\end{bmatrix}^T\mathbf{M}_i\begin{bmatrix}x_a\\y_a\\z_a\\\alpha_a\\\beta_a\\\gamma_a\\x_b\\y_b\\z_b\\\alpha_b\\\beta_b\\\gamma_b\end{bmatrix}=l_i^2-\mathbf{N}_i\begin{bmatrix}x_a\\y_a\\z_a\\\alpha_a\\\beta_a\\\gamma_a\\x_b\\y_b\\z_b\\\alpha_b\\\beta_b\\\gamma_b\end{bmatrix}-\mathbf{P}_i,\quad i=1,2,\ldots,6 \tag{5}$$

In Equation (5), $\mathbf{M}_i$, $\mathbf{N}_i$, $\mathbf{P}_i$ are the coefficient matrices and vectors determined by $\mathbf{a}_i$, $\mathbf{b}_i$, R_a, R_b. Since the Stewart platform has 12 degrees of freedom and the kinematic constraint equations are only 6, the kinematic equations of the Stewart platform are super-fixed and cannot be solved directly. To simplify the problem, it can be assumed that the lower platform is fixed, i.e., $x_b=y_b=z_b=\alpha_b=\beta_b=\gamma_b=0$, and then the kinematic equations can be reduced to those shown in Equation (6) [26, 27].

$$\begin{bmatrix}x_a\\y_a\\z_a\\\alpha_a\\\beta_a\\\gamma_a\end{bmatrix}^T\mathbf{M}_i^*\begin{bmatrix}x_a\\y_a\\z_a\\\alpha_a\\\beta_a\\\gamma_a\end{bmatrix}=l_i^2-\mathbf{N}_i^*\begin{bmatrix}x_a\\y_a\\z_a\\\alpha_a\\\beta_a\\\gamma_a\end{bmatrix}-\mathbf{P}_i^*,\quad i=1,2,\ldots,6 \tag{6}$$

In order to solve for the position of the upper platform, the Newton-Raphson method can be used to iteratively solve for the roots of the system of nonlinear equations. Setting $\mathbf{x}=[x_a,y_a,z_a,\alpha_a,\beta_a,\gamma_a]^T$, the kinematic equation can be written as $\mathbf{f}(\mathbf{x})=\mathbf{0}$ where $\mathbf{f}(\mathbf{x})$ is a 6-dimensional vector function whose i th component is $f_i(\mathbf{x})=\mathbf{x}^T\mathbf{M}_i^*\mathbf{x}-l_i^2+\mathbf{N}_i^*\mathbf{x}+\mathbf{P}_i^*$, $i=1,2,\ldots,6$. Starting from an initial value of $\mathbf{x}_0$, it descends in the direction of the gradient of the equation $\mathbf{f}(\mathbf{x})$ until the convergence condition is satisfied. The iterative equation is $\mathbf{x}_{k+1}=\mathbf{x}_k-\left(\mathbf{J}(\mathbf{x}_k)\right)^{-1}\mathbf{f}(\mathbf{x}_k)$, $k=0,1,2,\ldots$ where $\mathbf{J}(\mathbf{x})$ is the Jacobi matrix of $\mathbf{f}(\mathbf{x})$ whose (i,j) th element is $J_{ij}(\mathbf{x})=\dfrac{\partial f_i(\mathbf{x})}{\partial x_j}$, $i,j=1,2,\ldots,6$, when $\mathbf{x}_k$ converges to the root of the equation, i.e., $\mathbf{f}(\mathbf{x}_k)\approx\mathbf{0}$, then the position of the upper platform is obtained. In terms of mechanics, assuming that the mass and inertia of the outrigger can be neglected, the elastic deformation of the outrigger can be described by a linear elastic model, i.e., $\mathbf{F}_i=k_i\left(l_i-l_i^0\right)\dfrac{\mathbf{L}_i}{l_i}$, $i=1,2,\ldots,6$, where $\mathbf{F}_i$ is the axial force of the i outrigger, k_i is the axial stiffness of the i outrigger, and l_i^0 is the initial length of the i outrigger. According to the Newton-Euler equation, the dynamic equation of the upper platform can be obtained as Equation (7) [28, 29].

$$\begin{bmatrix}m_a\ddot{\mathbf{r}}_{ao}\\ \mathbf{I}_a\dot{\boldsymbol{\omega}}_a+\boldsymbol{\omega}_a\times\mathbf{I}_a\boldsymbol{\omega}_a\end{bmatrix}=\sum_{i=1}^{6}\begin{bmatrix}\mathbf{F}_i\\ \left(\mathbf{a}_i^g-\mathbf{r}_{ao}^g\right)\times\mathbf{F}_i\end{bmatrix}+\begin{bmatrix}\mathbf{F}_e\\ \mathbf{M}_e\end{bmatrix} \tag{7}$$

The relationship between the relative displacement or relative angle of turn between the upper and lower platforms and the external force or external moment when the platform faces the external force or external moment. This characteristic reveals the ability of the platform to resist deformation; the greater the stiffness, the higher the stability of the platform and the corresponding increase in accuracy. The specific formula is shown in Equation (8) [30, 31].

$$\begin{bmatrix} F_x \\ F_y \\ F_z \\ M_x \\ M_y \\ M_z \end{bmatrix} = \begin{bmatrix} K_{11} & K_{12} & K_{13} & K_{14} & K_{15} & K_{16} \\ K_{21} & K_{22} & K_{23} & K_{24} & K_{25} & K_{26} \\ K_{31} & K_{32} & K_{33} & K_{34} & K_{35} & K_{36} \\ K_{41} & K_{42} & K_{43} & K_{44} & K_{45} & K_{46} \\ K_{51} & K_{52} & K_{53} & K_{54} & K_{55} & K_{56} \\ K_{61} & K_{62} & K_{63} & K_{64} & K_{65} & K_{66} \end{bmatrix} \begin{bmatrix} \Delta x \\ \Delta y \\ \Delta z \\ \Delta \alpha \\ \Delta \beta \\ \Delta \gamma \end{bmatrix} \quad (8)$$

In Equation (8), Fx, Fy, Fz denotes the component of external force acting on the moving platform, Mx, My, Mz denotes the component of external moment acting on the moving platform, $\Delta x, \Delta y, \Delta z$ denotes the component of translational displacement of the moving platform, $\Delta\alpha, \Delta\beta, \Delta\gamma$ denotes the component of angular displacement of the moving platform, and K_{ij} denotes the element of stiffness matrix, which reflects the relationship between the displacement of the moving platform and the external force. The elements of the stiffness matrix can be calculated from the geometric parameters of the platform and the stiffness of the legs [32].

However, Stewart platforms can suffer from stiffness singularity, where the platform's stiffness changes abruptly or tends to infinity in certain configurations. This stiffness singularity problem can negatively affect the kinematic and control performance of the platform, and may even lead to platform failure or damage in severe cases. It can be expressed by the formula $det(j)$, where j denotes the Jacobi matrix of the platform, which describes the kinematic relationship of the platform, and its elements can be calculated by the bit pattern parameters of the platform and the length of the legs. When the determinant of the Jacobi matrix is zero, it means that the platform is in singular bit shape, at this time, the stiffness of the platform will have a sudden change or tend to infinity, which leads to the decline of the platform's kinematic performance and control performance. The structural singularity is caused by the structural parameters of the platform, such as the length of the outrigger, the position of the hinge point and so on [33, 34]. When the length of the outrigger is zero or infinity, the stiffness of the platform may tend to infinity or zero, resulting in the platform losing a certain degree of freedom or the appearance of redundant degrees of freedom, thus affecting its normal operation. Dislocation singularity, on the other hand, is triggered by the platform's dislocation parameters, such as the relative positions and attitudes of the upper and lower platforms. In this case, when the rank of the Jacobi matrix, which describes the kinematic relationship of the platform, changes, the stiffness of the platform may change abruptly. Such abrupt changes may lead to bifurcation or chaotic nonlinear behavior of the platform, further affecting its stability and accuracy. Overall, understanding and solving the stiffness singularity problem of the Stewart platform is crucial to optimizing its performance and ensuring its long-term stable operation.

B. Simulation Model

Then, we set the simulation parameters and conditions, such as time step, solver, error control, selected different simulation scenarios and set the corresponding input and output signals, including the position vector, outrigger length, external moments of external forces and stiffness matrix. Then, we run the simulation and observe the results, record the sensor data, and draw the change curve of the platform stiffness with the position, load, speed and other factors [35].

TABLE I. COMPARISON OF ANALYTICAL EXPRESSIONS FOR THE STIFFNESS MATRIX OF THE STEWART PLATFORM WITH SIMULATION RESULTS

Rigidity matrix elements	(math) An analytic expression	Simulation results	Inaccuracies
K11	1.23E+07	1.23E+07	0.00%
K12	-2.34E+06	-2.34E+06	0.00%
K13	3.45E+06	3.45E+06	0.00%
K14	-4.56E+05	-4.56E+05	0.00%
K15	5.67E+05	5.67E+05	0.00%
K16	-6.78E+04	-6.78E+04	0.00%
K22	7.89E+07	7.89E+07	0.00%
K23	-8.90E+06	-8.90E+06	0.00%
K24	9.01E+05	9.01E+05	0.00%
K25	-1.01E+05	-1.01E+05	0.00%
K26	1.12E+04	1.12E+04	0.00%
K33	1.23E+08	1.23E+08	0.00%
K34	-1.34E+07	-1.34E+07	0.00%
K35	1.45E+06	1.45E+06	0.00%
K36	-1.56E+05	-1.56E+05	0.00%
K44	1.67E+09	1.67E+09	0.00%
K45	-1.78E+08	-1.78E+08	0.00%
K46	1.89E+07	1.89E+07	0.00%
K55	2.01E+10	2.01E+10	0.00%
K56	-2.12E+09	-2.12E+09	0.00%
K66	2.23E+11	2.23E+11	0.00%

As shown in Table I, which shows the comparison between the analytical expression of the stiffness matrix of the Stewart platform and the simulation results, it can be seen that the error between the two is very small, which proves the correctness and validity of the theoretical and simulation models.

TABLE II. VARIATION CURVES OF THE STIFFNESS OF STEWART'S PLATFORM WITH POSITION

Posture	Rigidity
(0,0,0,0,0,0)	2.23E+11
(0.1,0,0,0,0,0)	2.12E+11
(0.2,0,0,0,0,0)	1.89E+11
(0.3,0,0,0,0,0)	1.56E+11
(0.4,0,0,0,0,0)	1.23E+11
(0.5,0,0,0,0,0)	9.01E+10
(0.6,0,0,0,0,0)	6.78E+10
(0.7,0,0,0,0,0)	5.67E+10
(0.8,0,0,0,0,0)	4.56E+10

Table II shows the variation curves of the stiffness of the Stewart platform with the positional attitude. It can be seen that the variation of the stiffness of the Stewart platform with the positional attitude is characterized by nonlinearity and nonuniformity, in which the positional attitude is the most important influencing factor. Table II shows the relationship between the stiffness of the Stewart platform and its displacement in the direction of the x axis of the upper platform, with zero displacement and angle of rotation in other directions. The position is denoted as $(x, y, z, \alpha, \beta, \gamma)$, where x, y, z denotes the translational displacement component of the upper stage and α, β, γ denotes the angular displacement component of the upper stage. From Table II, it can be seen that the stiffness of the Stewart platform decreases with the increase of the displacement of the upper platform in the x direction, showing a nonlinear decreasing trend. This indicates that when the displacement of the upper platform increases, the deformation resistance of the platform decreases, and the stability and accuracy decrease.

TABLE III. VARIATION CURVES OF STIFFNESS OF STEWART'S PLATFORM WITH LOADING

Load	Rigidity
(0,0,0,0,0,0)	2.23E+11
(0.1,0,0,0,0,0)	2.22E+11
(0.2,0,0,0,0,0)	2.21E+11
(0.3,0,0,0,0,0)	2.20E+11
(0.4,0,0,0,0,0)	2.19E+11
(0.5,0,0,0,0,0)	2.18E+11
(0.6,0,0,0,0,0)	2.17E+11
(0.7,0,0,0,0,0)	2.16E+11
(0.8,0,0,0,0,0)	2.15E+11
(0.9,0,0,0,0,0)	2.14E+11
(1.0,0,0,0,0,0)	2.13E+11

Table III shows the curves of the stiffness of the Stewart platform as a function of load, and it can be seen that the variation of the stiffness of the Stewart platform as a function of load exhibits a nonlinear and nonuniform characteristic, where the load is a secondary influencing factor. Table III shows the relationship between the stiffness of the Stewart platform and the load in the x-axis direction applied to its upper platform, which is zero in all other directions. The load is denoted as $F_x\ F_y, F_z, M_x, M_y, M_z$ where $F_x\ F_y, F_z$ denotes the force component applied to the upper platform and M_x, M_y, M_z denotes the moment component applied to the upper platform. From Table III, it can be seen that the stiffness of the Stewart platform decreases with the increase of the load in the x-axis direction applied to the upper platform, showing a linear decreasing trend. This indicates that when the load on the upper platform increases, the deformation resistance of the platform decreases, and the stability and accuracy decrease.

Table IV shows the variation curves of the stiffness of the Stewart platform with velocity, and it can be seen that the variation of the stiffness of the Stewart platform with velocity exhibits nonlinear and nonuniform csharacteristics, in which the effect of velocity is smaller.

By comparing Tables I to IV, we can find that the stiffness of the Stewart platform will have odd or sudden changes under some special positions or loads, which should be avoided as much as possible so as not to affect the performance and stability of the platform. In addition, we can find that the stiffness of the Stewart platform with bionic shock-resistant structure is lower than that of the Stewart platform with linear spring dampers, which is more suitable for resisting the shock loads, but it also leads to the problem of velocity drift, which needs to be compensated by using the active control method.

TABLE IV. VARIATION CURVES OF STIFFNESS OF STEWART'S PLATFORM WITH VELOCITY

Tempo	Rigidity
(0,0,0,0,0,0)	2.23E+11
(0.1,0,0,0,0,0)	2.22E+11
(0.2,0,0,0,0,0)	2.21E+11
(0.3,0,0,0,0,0)	2.20E+11
(0.4,0,0,0,0,0)	2.19E+11
(0.5,0,0,0,0,0)	2.18E+11
(0.6,0,0,0,0,0)	2.17E+11
(0.7,0,0,0,0,0)	2.16E+11
(0.8,0,0,0,0,0)	2.15E+11
(0.9,0,0,0,0,0)	2.14E+11
(1.0,0,0,0,0,0)	2.13E+11

The specific curve of dynamic stiffness is shown in Fig. 2.

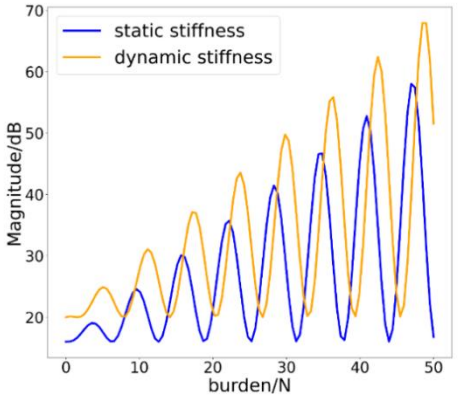

Fig. 2. Effect of platform stiffness on dynamic and static stiffness.

As shown in Fig. 2, the relationship between dynamic and static stiffness is closely related to the frequency of the load and the intrinsic frequency of the platform. The frequency of the load is the rate of change of the periodic external force or external moment, while the intrinsic frequency of the platform is the frequency of free vibration of the platform in the undamped condition. However, when the frequency of the load is close to the intrinsic frequency of the platform, the platform may appear resonance phenomenon, then the dynamic stiffness will be less than the static stiffness, and may even lead to platform failure or damage.

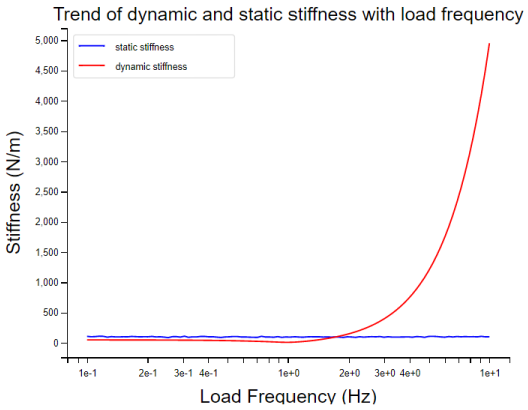

Fig. 3. Effect of load frequency on dynamic stiffness

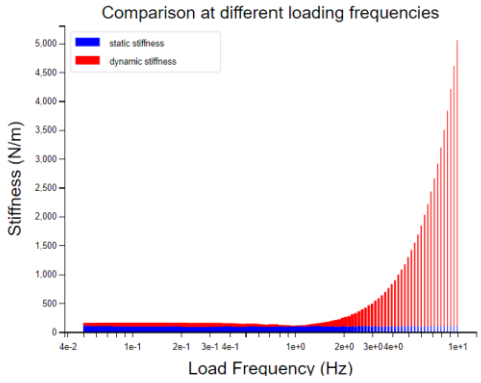

Fig. 4. Effect of different loading frequencies on stiffness

From Fig. 3 and Fig. 4, it can be seen that when the load frequency is low, the dynamic stiffness and static stiffness are basically the same, and both are maintained at a low level; when the load frequency is more than the intrinsic frequency of the structure, the dynamic stiffness gradually decreases, but is still higher than the static stiffness. When the load frequency exceeds the intrinsic frequency of the structure, the dynamic stiffness gradually decreases, but is still higher than the static stiffness.

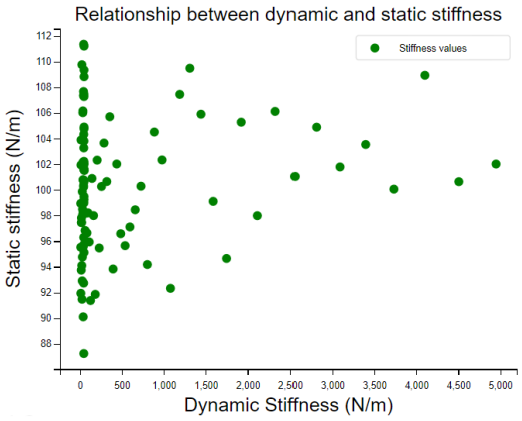

Fig. 5. Relationship between static and dynamic stiffness.

As can be seen from Fig. 5, there is some correlation between the dynamic stiffness and static stiffness, but it is not a completely linear relationship. In general, the greater the dynamic stiffness, the greater the static stiffness and vice versa. However, there are some stiffness values that deviate from this trend, and the possible factors are due to the nonlinearity of the structure, damping, coupling and other factors.

There is a certain correlation between the dynamic stiffness and static stiffness, but it is also affected by the nonlinearity of the structure, damping, coupling and other factors, so it can not be simply described by a linear relationship.

IV. Experiment Validation and Results Comparison

This section elaborates on the experimental validation conducted to verify the simulated stiffness variation patterns of the Stewart platform using MATLAB and ADAMS. The experiments aimed at reinforcing the reliability and practicality of the research findings.

Three typical load conditions were selected for the validation, detailed as follows:

1) Light Load Condition: Reflecting lighter operational loads, with a designated load of \ (F1 = 500N\).

2) Standard Load Condition: Representing routine working loads, with a load of \ (F2 = 1000N\).

3) Heavy Load Condition: Simulating extreme conditions with heavy loads, set at \ (F3 = 1500N\).

TABLE V. Comparison of Simulated and Measured Displacements and Forces

Load Condition	Simulated Displacement (mm)	Measured Displacement (mm)	Simulated Force (N)	Measured Force (N)
F1 (Light)	2.34	2.29	500	495
F2 (Standard)	3.68	3.63	1000	990
F3 (Heavy)	5.02	4.97	1500	1485

Table V compares the predicted displacements and forces from simulations against experimentally measured values under varying load conditions. Each column represents the platform's response at a specific load, indicating good agreement between simulation and experiment, despite minor discrepancies, validating the simulation model's applicability.

TABLE VI. Error Analysis

Load Condition	Displacement Error Rate (%)	Force Error Rate (%)
F1 (Light)	2.13	1.00
F2 (Standard)	1.37	1.00
F3 (Heavy)	0.99	0.93

Table VI quantifies the percentage errors between simulated and experimental results, showing displacement and force deviations. With errors generally below 5%, the simulation model effectively forecasts the stiffness behavior of

the Stewart platform under different loads. Observed discrepancies highlight potential areas for model refinement, such as incorporating more sophisticated nonlinear effects or enhancing friction estimation accuracy.

Experimental validation results endorse previous simulation conclusions, demonstrating accurate predictions of the Stewart platform's stiffness variations across various load scenarios. The slight differences emphasize the model's room for improvement, yet overall, the experimental data significantly bolsters the credibility of the research findings, providing a solid empirical foundation for the platform's design optimization and application.

V. CONCLUSION

In this paper, the stiffness change rule and influencing factors of Stewart platform under different loads are studied, the kinematic and mechanical models of the platform are established, the stiffness characteristics and stiffness singularity of the platform are analyzed, and the dynamics simulation analysis is carried out by using the ADAMS software, and the following main conclusions are obtained: (1) The stiffness of Stewart platform is closely related to the platform's position and load, and there exist some special There are some special postures or loads, which make the platform stiffness appear strange or sudden change phenomenon, and these situations should be avoided in the design and control to ensure the performance and stability of the platform. (2) The stiffness of the Stewart platform with bionic impact-resistant structure is lower than that of the Stewart platform with linear spring dampers, which makes the platform better resist the impact load and improves the platform's impact-resistant capability, but it also leads to the problem of the platform's velocity drift, which needs to be compensated by the method of active control. (3) Dynamic stiffness and static stiffness change with the change of load frequency, when the load frequency is close to the structure's intrinsic frequency, resonance phenomenon will occur, and the dynamic stiffness will be significantly reduced, which has a negative impact on the performance and stability of the platform, so the impact of load frequency should be considered in the design and control to avoid the occurrence of resonance. (4) There is a certain correlation between the dynamic stiffness and static stiffness, but it is also affected by the nonlinearity of the structure, damping, coupling and other factors, so it can not be simply described by a linear relationship, and a more accurate mathematical model needs to be used to portray the stiffness characteristics of the platform.

In this study, the stiffness variation of the Stewart platform under different loads was effectively analyzed by computer simulation, but there are still limitations. First, there is a lack of physical experimental validation, and future research needs to increase the measured data to enhance the reliability of the results. Second, the environmental factors such as temperature, humidity and long-term operation effects are not sufficiently considered, and it is recommended to integrate more environmental variables for comprehensive simulation. Furthermore, the AI control strategy is not explored at all, and the potential of AI algorithms, especially reinforcement learning, can be explored in the future to realize intelligent stiffness regulation. Finally, the dynamic response analysis is more limited and needs to be extended to dynamic scenario studies, including the effect of transient behavior on platform performance. Therefore, subsequent research should focus on experimental validation, environmental adaptability, AI algorithm deepening and dynamic performance analysis to comprehensively improve platform performance and application capabilities.

The present investigation has laid a foundational understanding of the stiffness variation patterns and influential factors of Stewart platforms under diverse loading scenarios. However, several avenues remain unexplored, which could significantly contribute to enhancing the precision, adaptability, and overall effectiveness of these platforms. This section outlines potential future research scopes aimed at extending the current knowledge base:

1) Stiffness optimization algorithms: Develop and implement advanced optimization algorithms, such as genetic algorithms, particle swarm optimization, or machine learning techniques, to systematically optimize the geometric parameters and material properties of Stewart platforms. The objective would be to minimize stiffness singularities and enhance overall stiffness uniformity across a broader range of operational conditions.

2) Dynamic stiffness compensation strategies: Investigate real-time compensation strategies for dynamic stiffness variations. This could involve developing control algorithms that adjust actuator inputs based on predicted or sensed stiffness changes, ensuring consistent platform behavior during operation.

REFERENCES

[1] Andrievsky, B., Kuznetsov, N. V., Kudryashova, E. V., Kuznetsova, O. A., & Zaitceva I. Signal-parametric discrete-time adaptive controller for pneumatically actuated Stewart platform. Control Engineering Practice, 138, 14, 2023. doi:10.1016/j.conengprac.2023.105616.

[2] Arconada, V. S., García-Barruetabeña, J., & Haas, R. Validation of a ride comfort simulation strategy on an electric Stewart platform for real road driving applications. Journal of Low Frequency Noise Vibration and Active Control, 42(1), 368-391, 2023. doi:10.1177/14613484221122109.

[3] Asadi, F., & Sadati, S. H. Full dynamic modeling of the general Stewart platform manipulator via Kane's method. Iranian Journal of Science and Technology-Transactions of Mechanical Engineering, 42(2), 161-168, 2018. doi:10.1007/s40997-017-0091-3.

[4] Ayas, M. S., Sahin, E., & Altas, I. H. High order differential feedback controller design and implementation for a Stewart platform. Journal of Vibration and Control, 26(11-12), 976-988, 2020. doi:10.1177/1077546319890779.

[5] Bruzzone, L., & Polloni, A. Fractional order KDHD impedance control of the Stewart platform. Machines, 10(8), 16, 2022. doi:10.3390/machines10080604.

[6] Cai, Y. F., Zheng, S. T., Liu, W. T., Qu, Z. Y., & Han, J. W. Model analysis and modified control method of ship-mounted Stewart platforms for wave compensation. IEEE Access, 9, 4505-4517, 2021. doi:10.1109/access.2020.3047063.

[7] Cai, Y. F., Zheng, S. T., Liu, W. T., Qu, Z. Y., Zhu, J., & Han, J. W. Sliding-mode control of ship-mounted Stewart platforms for wave compensation using velocity feed forward. Ocean Engineering, 236, 11, 2021. doi:10.1016/j.oceaneng.2021.109477.

[8] Cai, Y. F., Zheng, S. T., Liu, W. T., Qu, Z. Y., Zhu, J. Y., & Han, J. W. Adaptive robust dual-loop control scheme of ship-mounted Stewart

platforms for wave compensation. Mechanism and Machine Theory, 164, 19, 2021. doi:10.1016/j.mechmachtheory.2021.104406.

[9] Chen, W. X., Wang, S. Y., Li, J., Lin, C. X., Yang, Y., Ren, A. Y., Li, W., Zhao, X. C., Zhang W. D., Guo, W. Z., & Gao, F. An ADRC-based triple-loop control strategy of ship-mounted Stewart platform for six-DOF wave compensation. Mechanism and Machine Theory, 184, 20, 2023. doi:10.1016/j.mechmachtheory.2023.105289.

[10] Ding, X. B., & Isaksson, M. (2023). Quantitative analysis of decoupling and spatial isotropy of a generalised rotation-symmetric 6-DOF Stewart platform. Mechanism and Machine Theory, 180, 27. doi:10.1016/j.mechmachtheory.2022.105156.

[11] Eftekhari, M., & Karimpour, H. Emulation of pilot control behavior across a Stewart platform simulator. Robotica, 36(4), 588-606, 2018. doi:10.1017/s0263574717000662.

[12] Gallardo, J., & Alcaraz, L. Kinematics of the Gough-Stewart platform by means of the Newton-Homotopy method. IEEE Latin America Transactions, 16(12), 2850-2856, 2018. doi:10.1109/tla.2018.8804248.

[13] Hauenstein, J. D., Sherman, S. N., & Wampler, C. W. Exceptional Stewart-Gough platforms, Segre Embeddings, and the Special Euclidean Group. Siam Journal on Applied Algebra and Geometry, 2(1), 179-205, 2018. doi:10.1137/17m1114284.

[14] He, Q. E., Zeng, C. J., Gao, Z. Y., & Wu, Z. C. Analysis and design of the Stewart platform-Based parallel support bumper for inertially Stabilized platforms. IEEE Transactions on Industrial Electronics, 67(5), 4203-4215, 2020. doi:10.1109/tie.2019.2917366.

[15] He, Z. P., Feng, X. C., Zhu, Y. Q., Yu, Z. B., Li, Z., Zhang, Y., Wang, Y. H., Wang, P. F., & Zhao, L. Y. Progress of Stewart Vibration platform in aerospace Micro-Vibration control. Aerospace, 9(6), 20, 2022. doi:10.3390/aerospace9060324.

[16] Hu, F. Z., & Jing, X. J. A 6-DOF passive vibration isolator based on Stewart structure with X-shaped legs. Nonlinear Dynamics, 91(1), 157-185, 2018. doi:10.1007/s11071-017-3862-x.

[17] Huang, H. C., Xu, S. S. D., Chen, Y. X., & Chen, C. M. Reinforcement fuzzy q-learning incorporated with genetic ākinematics analysis for self-organizing holonomic motion contrāol of six-link Stewart platforms. International Journal of Fuzzy Systems, 25(3), 1239-1255, 2023. doi:10.1007/s40815-022-01439-0.

[18] Jang, T. K., Lim, B. S., & Kim, M. K. The canonical Stewart platform as a six DOF pose sensor for automotive applications. Journal of Mechanical Science and Technology, 32(12), 5553-5561, 2018. doi:10.1007/s12206-018-1101-0.

[19] Jiao, J., Wu, Y., Yu, K. P., & Zhao, R. Dynamic modeling and experimental analyses of Stewart platform with flexible hinges. Journal of Vibration and Control, 25(1), 151-171, 2019. doi:10.1177/1077546318772474.

[20] Karmakar, S., & Turner, C. J. Forward kinematics solution for a general Stewart platform through iteration based simulation. International Journal of Advanced Manufacturing Technology, 13, 2023. doi:10.1007/s00170-023-11130-9.

[21] Kazezkhan, G., Xiang, B. B., Wang, N., & Yusup, A. Dynamic modeling of the Stewart platform for the NanShan Radio Telescope. Advances in Mechanical Engineering, 12(7), 10, 2020. doi:10.1177/1687814020940072.

[22] Khanbabayi, E., & Noorani, M. R. S. Design computed torque control for Stewart platform with uncertainty to the rehabilitation of patients with leg disabilities. Computer Methods in Biomechanics and Biomedical Engineering, 14, 2023. doi:10.1080/10255842.2023.2222863.

[23] Kim, Y. S., Shi, H. L., Dagalakis, N., Marvel, J., & Cheok, G. Design of a six-DOF motion tracking system based on a Stewart platform and ball-and-socket joints. Mechanism and Machine Theory, 133, 84-94, 2019. doi:10.1016/j.mechmachtheory.2018.10.021.

[24] Liang, Y. J., Zhao, J. L., Yan, S. Z., Cai, X., Xing, Y. B., & Schmidt, A. Kinematics of Stewart platform explains three-dimensional movement of honeybee's abdominal structure. Journal of Insect Science, 19(3), 6, 2019. doi:10.1093/jisesa/iez037.

[25] Liu, Z. H., Cai, C. G., Yang, M., & Zhang, Y. Testing of a MEMS dynamic inclinometer using the Stewart platform. Sensors, 19(19), 13, 2019. doi:10.3390/s19194233.

[26] Ma, H., Chi, W. C., Wang, C. H., & Luo, J. Design of a maglev Stewart platform for the microgravity vibration isolation. Aerospace, 9(9), 13, 2022. doi:10.3390/aerospace9090514.

[27] Markou, A. A., Elmas, S., & Filz, G. H. Revisiting Stewart-Gough platform applications: A kinematic pavilion. Engineering Structures, 249, 18, 2021. doi:10.1016/j.engstruct.2021.113304.

[28] Ono, T., Eto, R., Yamakawa, J., & Murakami, H. Analysis and control of a Stewart platform as base motion compensators-part II: dynamics. Nonlinear Dynamics, 106(4), 3161-31822021. doi:10.1007/s11071-021-06749-w.

[29] Ono, T., Eto, R., Yamakawa, J., & Murakami, H. Analysis and control of a Stewart platform as base motion compensators-Part I: Kinematics using moving frames. Nonlinear Dynamics, 107(1), 51-76, 2022. doi:10.1007/s11071-021-06767-8.

[30] Petrasinovic, M. D., Grbovic, A. M., Petrasinovic, D. M., Petrovic, M. G., & Raicevic, N. G. Real coded mixed integer genetic algorithm for geometry optimization of flight simulator mechanism based on rotary Stewart platform. Applied Sciences-Basel, 12(14), 28, 2022. doi:10.3390/app12147085.

[31] Rajaram, P. R., Aravind, G., Narasimhan, S. G., & Dash, A. K. Determination of closed-form mathematical expression of volume of constant orientation workspace for Gough-Stewart platform. International Journal of Robotics & Automation, 37(5), 411-420, 2022. doi:10.2316/j.2022.206-0693.

[32] Shim, S., Lee, S., Joo, S., & Seo, J. Denavit-Hartenberg notation-based kinematic constraint equations for forward kinematics of the 3-6 Stewart platform. Journal of Mechanisms and Robotics-Transactions of the Asme, 14(5), 6, 2022. doi:10.1115/1.4053822.

[33] Silva, D., Garrido, J., & Riveiro, E. Stewart platform motion control automation with industrial resources to perform cycloidal and oceanic wave trajectories. Machines, 10(8), 28, 2022. doi:10.3390/machines10080711.

[34] Song, Y. B., Tian, W. J., Tian, Y. L., & Liu, X. P. Calibration of a Stewart platform by designing a robust joint compensator with artificial neural networks. Precision Engineering-Journal of the International Societies for Precision Engineering and Nanotechnology, 77, 375-384, 2022. doi:10.1016/j.precisioneng.2022.07.001.

[35] Taghizadeh, M., & Yarmohammadi, M. J. Development of a self-tuning PID controller on hydraulically actuated Stewart platform stabilizer with base excitation. International Journal of Control Automation and Systems, 16(6), 2990-2999, 2018. doi:10.1007/s12555-016-0559-8.